American Mineralogist, Volume 73, pages 568–584, 1988

XRD, FTIR, and TEM studies of optically anisotropic grossular garnets

Fred M. Allen*
Department of Geology, Arizona State University, Tempe, Arizona 85287, U.S.A.
Peter R. Buseck
Departments of Geology and Chemistry, Arizona State University, Tempe, Arizona 85287, U.S.A.

Abstract

Optical birefringence is common in calcic garnets, especially in those associated with contact metasomatic and hydrothermal ore deposits. Such garnets are noncubic, although their departure from cubic symmetry may be extremely slight. A number of suggestions have been made to explain the birefringence, but none serves as a general solution to the problem.

We have used a variety of techniques to examine sector-twinned, anisotropic, near-end-member grossular garnets from Eden Mills, Vermont ($Gr_{90}And_6Alm_4$), and Asbestos, Quebec ($Gr_{99}And_1$). XRD results show Al-Fe^{3+} ordering on the octahedral positions and Ca-Fe^{2+} ordering on the dodecahedral positions in the Eden Mills garnet. After annealing at 870 °C for 40 h, the sample becomes disordered and loses its birefringence. FTIR spectroscopy shows a noncubic distribution of OH groups. Samples that lose their birefringence when heated to 870 °C no longer contain a detectable hydroxyl component. Those heated to 800 °C, however, also apparently lose their water content but remain anisotropic.

Sectors contain differently ordered arrangements of Al and Fe^{3+} on octahedral positions. Changes in the ordering scheme or degree of ordering take place during growth. Strain in the crystal results from lattice mismatch, thereby reducing the symmetry from cubic. Stacking faults and dislocations, identified using TEM, occur near the boundaries of differently ordered sectors and presumably result from the lattice mismatch.

Introduction

Optical, X-ray, and morphological measurements indicate that most garnets are cubic. Some garnets, however, are optically anisotropic. Any well-trained student of optical mineralogy knows that a cubic mineral is optically isotropic and so exhibits no birefringence in cross-polarized light. Hence, by definition, an optically anisotropic garnet cannot be cubic. The fact that X-ray and morphological measurements show many of these garnets to be cubic poses an intriguing problem—how should the symmetry be specified when different crystallographic methods yield different symmetries?

To avoid confusion, an operational statement should accompany a symmetry determination; e.g., the garnet is cubic to X-rays but triclinic to the optical microscope. Such statements are needed if a crystal is twinned or chemically zoned because the symmetry of an individual component can differ markedly from the symmetry of the bulk crystal, and the scale on which an observation is made then becomes important.

Some techniques are better than others for detecting slight structural or chemical perturbations that affect symmetry. Optical measurements are particularly sensitive to such changes; even slight distortions or the presence of impurities can produce complex sectoral or lamellar structures. A drawback of the optical microscope, however, is its limited resolution (0.2 μm at best). Techniques such as X-ray diffraction or transmission electron microscopy offer higher resolution, but these methods are difficult to use for measuring the effects of minor imperfections on symmetry.

One goal of the present study was to compare different crystallographic methods in their ability to detect a reduction from cubic symmetry in optically anisotropic garnets. Another goal was to determine the cause(s) of the symmetry reduction. Birefringence is observed in calcic garnets, especially grossular-andradite (grandite) garnets ($^{VIII}Ca_3{}^{VI}(Al,Fe^{3+})_2{}^{IV}Si_3O_{12}$) from skarns, hydrothermal ore deposits, and contact-metamorphic rocks. Thus, there appears to be a relationship between chemistry and birefringence. Various hypotheses have been proposed to account for the optical anisotropy, but none serves as a comprehensive solution. These hypotheses include (1) plastic deformation; (2) substitution of rare-earth ions for Ca, giving rise to magneto-optic effects (Blanc and Maisonneuve, 1973); (3) strain arising from lattice mismatch at subgrain, composition, or twin boundaries (Chase and Lefever, 1960; Lessing and Standish, 1973; Kitamura and Komatsu, 1978); (4) ordering of Al and Fe^{3+} on the oc-

* Current address: Engelhard Corporation, Research and Development, Menlo Park, CN 28, Edison, New Jersey 08818, U.S.A.

0003–004X/88/0506–0568$02.00

TABLE 1. Chemical analyses of grossular garnets examined in this study

	Asbestos, Quebec		Eden Mills, Vermont	
	Wt%	No. of ions	Wt%	No. of ions
SiO_2	39.83 (0.33)	3.00	39.37 (0.41)	3.00
Al_2O_3	22.29 (0.21)	1.98	21.06 (1.89)	1.89
Fe_2O_3	0.38*	0.02	1.92**	0.11
FeO	—		2.08	0.13
MnO	0.12 (0.03)	0.01	0.13 (0.05)	0.01
CaO	37.12 (0.28)	2.99	35.08 (0.48)	2.86
Sum	99.74	8.00	99.64	8.00
H_2O†	0.10		0.23	
	Mol% end members			
Gr		99.0		90.2
And		1.0		5.5
Alm		—		4.3

Note: Oxide weight percents were obtained with an electron microprobe. The average of 10 analyses are listed for each sample, with standard deviations given in parentheses.

* Total Fe was determined as "FeO" (0.34 ± 0.08 wt%) and converted to "Fe_2O_3" by multiplying by 1.1113 (= 79.85/71.85).

** Total Fe was determined as "FeO" (3.81 ± 0.37 wt%) and converted to Fe_2O_3 and FeO using the relations $3.81 = w_{FeO} + 0.8998(w_{Fe_2O_3})$ and $1.20 = 1.1113(w_{FeO}/w_{Fe_2O_3})$. The second equation is from the area ratio of Mössbauer doublets from Manning and Tricker (1977).

† Wt% H_2O from Manning and Tricker (1977), determined by wet-chemical analysis.

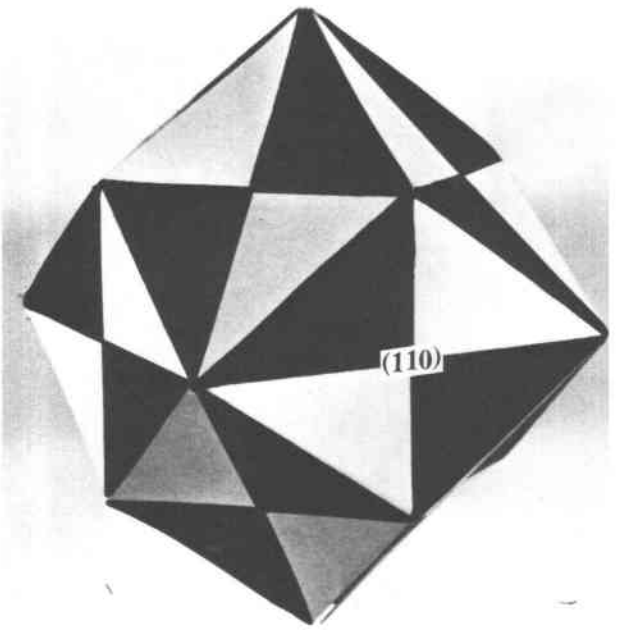

Fig. 1. Model illustrating sector twinning in a dodecahedral crystal of garnet. Shaded and unshaded areas on {110} faces represent sectors in slightly different optical orientations.

tahedral sites (Takéuchi et al., 1982); and (5) presence of OH groups distributed in a noncubic manner (Rossman and Aines, 1986). We tested the viability of some of these hypotheses. Our results impose constraints on the possible causes for the symmetry reduction, especially hypotheses 3, 4, and 5.

We used powder and single-crystal X-ray diffraction (XRD), Fourier transform infrared (FTIR) spectroscopy, and transmission electron microscopy (TEM) to investigate the origin of birefringence in garnet. To avoid the possible effects of strain produced by chemical zonation, our study was confined to the problem of birefringence in nearly pure gossulars.

Sample descriptions

Near-end-member grossulars occur in the rodingites associated with serpentinites at Belvidere Mountain, near Eden Mills, Vermont, and in Asbestos, Quebec. These rocks formed by metasomatism below 300 °C, on the basis of the presence of chrysotile-lizardite rather than antigorite + brucite (Evans et al., 1976). At both localities, euhedral crystals of garnet up to 1 cm in diameter line the walls of cavities and fractures in the rodingite. Diopside and vesuvianite may also be present. There is no evidence that the rodingites have been plastically deformed, so the crystals were probably not strained after growth. All optical properties and internal textures are therefore probably primary.

The Eden Mills grossular is orange with composition $Gr_{90}And_6Alm_4$. Chemical data are given in Table 1. Optical data suggest that crystals with perfect dodecahedral form consist of 48 pyramidal sectors with vertices meeting at the center (Fig. 1). Most of the crystals examined are intergrown portions of dodecahedra displaying only a few well-developed faces. Growth steps parallel to {211} are present on the {110} faces of many specimens (Fig. 2).

A thin section parallel to a {110} face reveals a "bow-tie" structure with four sectors (Fig. 3). Opposing sectors are related by twofold rotation and have the same extinction positions. Adjacent sectors are related by reflection across {100} and {110} planes and have different extinction positions (Figs. 4 and 5). Each sector contains lamellar features that correlate with the growth steps on the crystal surface.

The optical data presented here and by Akizuki (1984) show that the Eden Mills garnets have nearly monoclinic symmetry. Although there seems to be a twofold axis of rotation around the principal vibration axis, X, normal to the plane of the bow-tie, a comparison of lamellar features within opposing sectors reveals a breakdown of twofold symmetry. The orientation of X varies slightly within each sector, and, as a result, none of the three principal vibration axes actually coincides with an axis of symmetry. The conclusion, therefore, is that the Eden Mills garnets are optically triclinic.

The Asbestos grossular is colorless or tinted light brown with composition $Gr_{99}And_1$. Trapezohedron and hexoctahedron forms occur, both commonly exhibiting growth steps and etch pits. The sectoral structure is more complex than that in the Eden Mills garnet.

There is no major compositional difference between optically distinct sectors in both the Eden Mills and Asbestos garnets. Electron-microprobe traverses across ori-

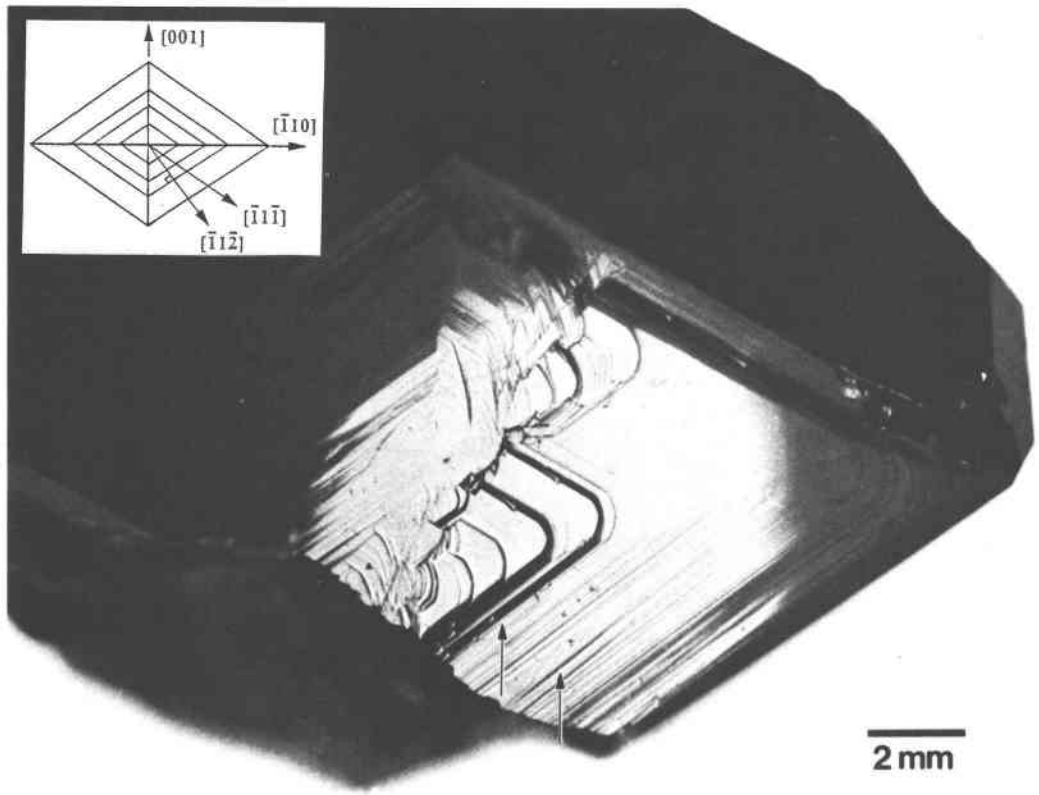

Fig. 2. Growth steps (arrows) on a {110} surface of Eden Mills grossular ($Gr_{90}And_6Alm_4$) seen in reflected light.

ented sections of Eden Mills garnet revealed no more than 5% variation in the Al:Fe ratio. In both the Eden Mills and Asbestos samples, ~0.1 wt% Mn was detected, and trace amounts of Na and Mg occur in the Eden Mills sample as shown by the ion probe.

Manning and Tricker (1977) reported a Fe^{2+}:Fe^{3+} ratio of 1.20 for an Eden Mills garnet based on Mössbauer results. The total Fe content of their garnet (3.7 wt% "FeO") is nearly identical to that of ours (3.81 wt% "FeO"); hence, this Fe^{2+}:Fe^{3+} ratio was adopted for our samples. They also detected 0.23 wt% H_2O by wet-chemical analysis for the Eden Mills garnet and 0.10 wt% for an Fe-bearing sample from Asbestos.

XRD RESULTS

We examined a powdered sample and a single-crystal fragment using XRD both before and after heating to determine the symmetry of the Eden Mills garnet and to deduce whether cation ordering is responsible for the optical anisotropy. The powdered sample was obtained by crushing a thick section of a garnet exhibiting the bow-tie structure. Data were collected in the 2θ range of 5–140° using graphite-monochromatized Cu$K\alpha$ radiation on a Rigaku DMAX-IIB diffractometer. An internal Si standard (SRM-640A) was used for calibration. The XRD profile of the unheated specimen shows no extra reflections, peak broadening, or splitting to suggest a reduction from cubic symmetry. A cubic lattice parameter of 11.8493(8) Å was refined from 92 reflections.

Crystals of Eden Mills grossular become almost completely isotropic, losing their sectoral structure and most of their birefringence, when annealed in air at 870 °C for 40 h and cooled to room temperature. This result agrees with that of Hariya and Kimura (1978) who reported that anisotropic garnets invert to an isotropic form between 800 and 950 °C.

The crystals also change color from orange to brown after prolonged heating, probably arising from the oxidation of Fe. The powder pattern of the annealed material is identical to that of the unheated sample, yielding a refined cubic lattice parameter of 11.8488(8) Å.

Powder XRD failed to show any evidence of a reduction from cubic symmetry in these birefringent garnets, but single-crystal XRD proved successful. A crystal fragment was extracted from a portion of an individual sector with uniform extinction. Precession photographs show no streaking, split diffraction maxima indicative of twinning, or violations of space group *Ia3d*. (See Hirai and Nakazawa, 1986, for an example where precession photographs do reveal the low symmetry of a grandite garnet.)

X-ray intensity data were collected for 3356 reflections from one-half of the reflection sphere. The crystal was

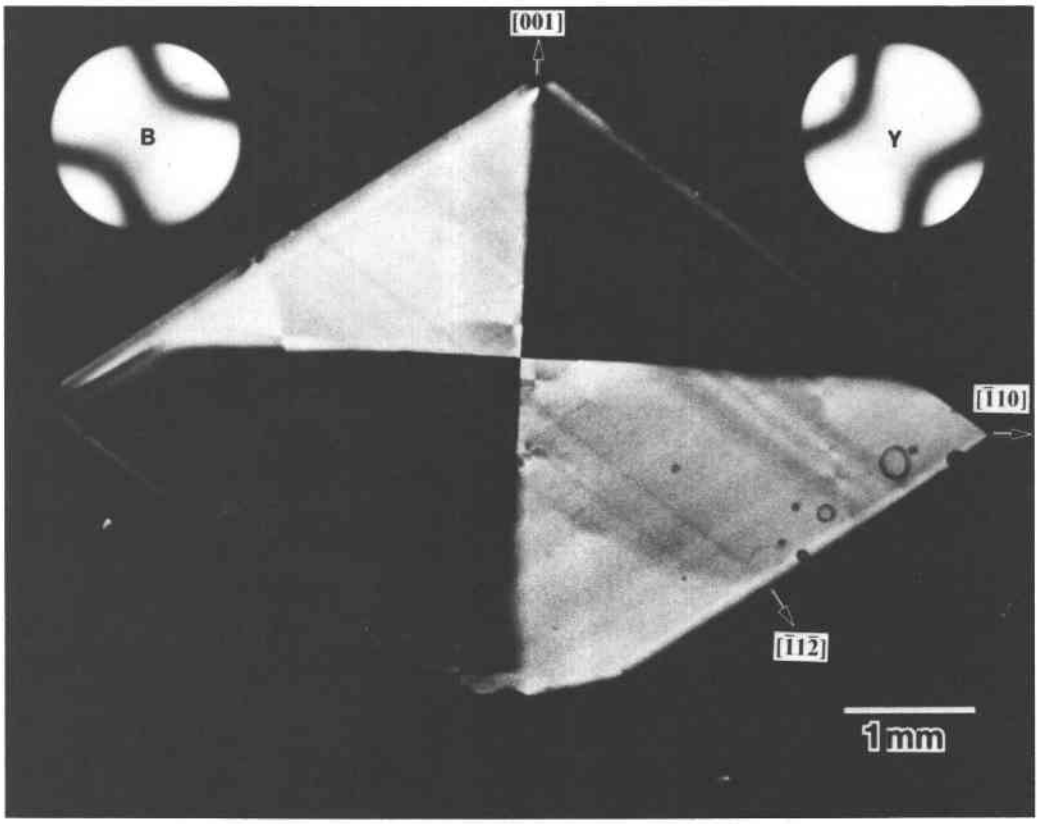

Fig. 3. [110] section of anisotropic garnet from Eden Mills displaying "bow-tie" structure (cross-polarized light). Interference figures from adjacent sectors are shown in the upper corners. B and Y stand for blue and yellow—the interference colors with the gypsum plate inserted.

then removed from its fiber, annealed at 870 °C, and quenched in air to room temperature. The crystal was optically isotropic following heating. After remounting in the same orientation as before heating, a second intensity data set consisting of 3339 reflections was collected over the same portion of reciprocal space. Details are given in Tables 2 and 3.

The unit-cell parameters before heating are consistent with the results of Takéuchi and Haga (1976), who de-

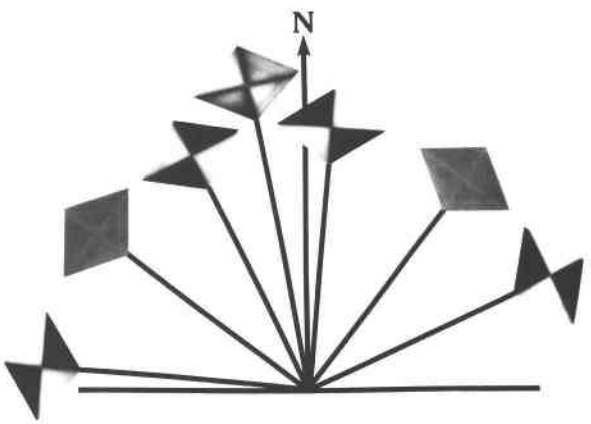

Fig. 4. Rotation of a [110] section of Eden Mills garnet in cross-polarized light. Sectors exhibit inclined extinction and are related by reflection twinning. N is the polarization direction of the analyzer.

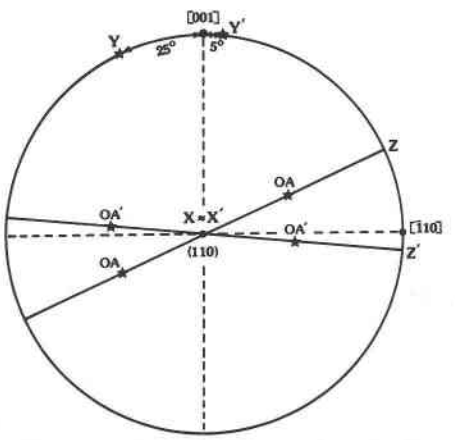

Fig. 5. Stereographic projection of the optical properties measured on a [110] thin section of Eden Mills grossular. Principal vibration directions of adjacent sectors are denoted X, Y, Z and X', Y', Z'. X and X' are almost normal to the (110) growth surface. Optic axes are indicated by OA and OA'. The $2V_Z$ value is about (+)80° in each sector.

TABLE 2. Crystal specifications for Eden Mills garnet

Size (mm)		0.25 × 0.23 × 0.19
Chemical composition		$Gr_{90.2}And_{5.5}Alm_{4.3}$
Color		Orange-brown
Maximum birefringence		~0.005
Cell dimensions*	Before heating	After heating
a (Å)	11.845(2)	11.837(2)
b	11.858(3)	11.840(3)
c	11.846(2)	11.836(3)
α (°)	89.98(2)	90.01(2)
β	89.96(1)	89.98(2)
γ	89.97(3)	90.00(2)
V (Å^3)	1663.9(6)	1658.8(7)
ρ_{calc} (g/cm^3)		3.64
μ (cm^{-1})		29.78
Transmission range		0.5664–0.6225

Note: Physical and chemical properties were measured on an anisotropic sample before heating.

* Cell dimensions are based on a least-squares refinement of angles for 15 reflections ($15° < 2\theta < 26°$). The numbers in parentheses are the standard deviations of the last figures.

TABLE 3. Instrument settings, data-acquisition parameters, and refinement results

Diffractometer	Syntex $P\bar{1}$
Radiation	Graphite-monochromatized Mo$K\alpha$
Tube settings	40 kV, 25 mA
Scan technique	θ–2θ
Scan range (°)	$2.0 + (2\theta_{K\alpha1} - 2\theta_{K\alpha2})$
Scan speed (°/min)	Variable 1–8
Ratio of total background time to scan time	0.25
Data collected	$\pm h, \pm k, +l$

		Before heating	After heating
Measured reflections*		5148**	5148†
Unique data with $F_o > 3\sigma_{F_o}$		3356	3339
Standard reflections††		3	3
Merging R factor (observed reflections)		5.49	2.09
Instrument instability factor, P		0.010	0.009
Space group‡			
$Ia3d$	R (%)	4.81	3.76
	R_w (%)	4.97	4.70
	n_{var}§	9	9
$I\bar{1}$	R (%)	4.21	3.53
	R_w (%)	4.55	4.36
	n_{var}	182	182

* All measured intensities were corrected for Lorentz and polarization effects for monochromatized radiation.

** 1565 unobserved reflections, 227 systematic absences for $Ia3d$.

† 1558 unobserved reflections, 251 systematic absences for $Ia3d$.

†† Standards were measured after every 100 reflections.

‡ Structure refinements were done with the program CRYSTALS. The atomic scattering factors for Ca, Al, Fe, Si, and O were taken from the *International Tables for X-ray Crystallography* (1974), with anomalous-dispersion corrections applied to each atom. The function minimized during all least-squares refinement processes was $\Sigma\, w(F_o - F_c)^2$, where $w = 1/\sigma_F^2$.

§ Includes scale factor and extinction parameter.

tected a monoclinic cell for garnet from Munam, Korea, with composition $Gr_{68}And_{32}$. After heating, the axes are more similar in length and the angles equal to 90° within error, consistent with cubic symmetry. The reduction in the unit-cell dimensions may be related to the expulsion of water from the structure.

The diffraction symmetry of the anisotropic garnet is determined by comparing reflections related by Laue symmetry $m3m$ (Fig. 6). Such a comparison also provides evidence for a structural change on heating. The intensity distribution before heating is consistent with Laue symmetry $\bar{1}$, whereas after heating, it is $m3m$.

The thin section from which the crystal was extracted was cut normal to the $[1\bar{1}0]$ axis of the X-ray cell. The principal vibration axis, X, is nearly parallel to $[1\bar{1}0]$ (Fig. 5). However, twofold rotational symmetry does not exist along $[1\bar{1}0]$, as shown by the distribution of diffracted intensities; numerous violations of Laue group $2/m$ are observed.

The structure of the Eden Mills garnet was refined both before and after heating in space groups $Ia3d$ and $I\bar{1}$ using the unmerged X-ray intensity data. In the $Ia3d$ structure, there is one dodecahedral X site (multiplicity, m = 24), one octahedral Y site (m = 16), one tetrahedral Z site (m = 24), and one anion O site (m = 96). In the $I\bar{1}$ structure, there are six X sites (m = 4), eight Y sites (m = 2), six Z sites (m = 4), and 24 O sites (m = 4). To maintain an Fe^{2+}:Fe^{3+} ratio of 1.20 in both structures, Ca and Fe were assigned to the 24 X positions per cell, with the total occupancy fixed at 22.95 Ca and 1.05 Fe; Al and Fe were assigned to the 16 Y positions with the total occupancy fixed at 15.12 Al and 0.88 Fe. Si was assigned to the 24 Z positions and O to the 96 anion positions. Isotropic temperature factors were used for all atoms in the refinements.

Optical second-harmonic analyses support the choice of $I\bar{1}$ by showing no evidence for the absence of a center of symmetry. Only the reflections allowed by space group $Ia3d$ were used in the refinement. No violations by body-centering were detected during data collection, but weak reflections violating screw-axis and glide-plane extinction criteria were observed both before and after heating. Psi-scans revealed that these weak reflections are a result of double diffraction.

The results of the X-ray structure refinements (Table 3) show that the unheated, anisotropic garnet refines better in space group $I\bar{1}$ than $Ia3d$. The improvement in R value is statistically significant at the 99.5% confidence level according to the Hamilton significance test. For the heated, isotropic crystal, the R values for the $I\bar{1}$ and $Ia3d$ refinements are nearly identical, suggesting that the structure is closer to cubic than before heating (Table 4). Tables of structure factors, atom positions, isotropic temperature factors, and bond lengths both before and after heating may be ordered.[1]

The occupancies of the X1 to X6 sites and Y1 to Y8 sites in the $I\bar{1}$ refinement for the anisotropic garnet show

[1] A copy of the deposited structural data may be ordered as Document AM-88-376 from the Business Office, Mineralogical Society of America, 1625 I Street, N.W., Suite 414, Washington, D.C. 20006, U.S.A. Please remit $5.00 in advance for the microfiche.

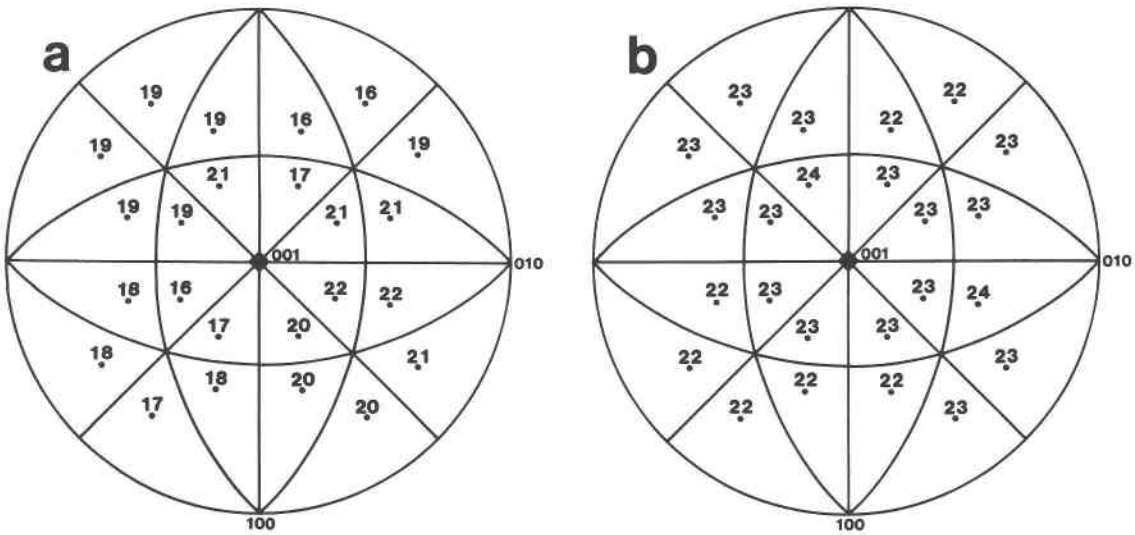

Fig. 6. Intensity distribution (corrected for absorption) of a set of 24 reflections of type 246; all should be equivalent for cubic garnet. (The actual intensities are 10^4 times the values indicated.) A measure of the variation in intensities of "equivalent" reflections is obtained by dividing the standard deviation by the average intensity for the set, yielding a coefficient of variation (CV). (**a**) Distribution for an anisotropic crystal of Eden Mills garnet. The Laue symmetry is $\bar{1}$, indicating a triclinic structure. The average intensity for this set of reflections is 19.0(1.8) × 10^4, CV = 9% (σ_{24} given in parentheses). (**b**) Distribution for the same crystal after annealing. The Laue symmetry is now $m3m$, with an average intensity of 22.8(0.5) × 10^4, CV = 2%.

partial ordering of Ca and Fe on the dodecahedral positions and Al and Fe on the octahedral positions. Comparison with isotropic garnet shows that disordering takes place with increasing temperature. Since the loss of birefringence accompanies this disordering, we conclude that the anisotropy is linked to substitutional ordering on the dodecahedral and octahedral positions. The same conclusion was reached by Takéuchi and co-workers for their intermediate grandite garnets (Takéuchi and Haga, 1976; Takéuchi et al., 1982).

The isotropic temperature factors for the six X and eight Y sites in the $I\bar{1}$ structure of the Eden Mills grossular range between 0.006 and 0.008 Å^2 both before and after heating. The uniformity of the temperature factors suggests that the occupancy variations are real and not an artifact of high correlations between parameters.

Positional ordering does not appear to be significant in causing optical anisotropy in garnet. Positions of atoms in the $I\bar{1}$ structure of the unheated crystal deviate by no more than 0.01 Å from their "ideal" positions in the $Ia3d$ structure. The same slight deviation from cubic symmetry was observed in the $I\bar{1}$ refinement for the isotropic sample.

FTIR RESULTS

Oriented sections of Eden Mills and Asbestos grossular were examined using FTIR spectroscopy to determine whether a low-symmetry distribution of OH groups could account for the optical anisotropy. Spectra were obtained on doubly polished, single-crystal slabs 100–200 μm thick. Data were collected at room temperature on a Nicolet 60SX FTIR spectrometer. Absorbances were corrected for specimen thickness. A 1-mm aperture was used to select the area of interest on each sample.

Unpolarized IR spectra (Figs. 7 and 8) reveal that (1) the absorption bands in the OH-stretching region are ori-

TABLE 4. Occupancies of dodecahedral (X) and octahedral (Y) sites in Eden Mills garnet before heating (anisotropic) and after heating (isotropic)

Site	m	Fe occupancy		
		Anisotropic		Isotropic
		Ia3d		
X	24	1.05	→	1.05
		$I\bar{1}$		
X1	4	0.16(4)	→	0.15(3)
X2	4	0.20(4)	→	0.14(3)
X3	4	0.10(4)	→	0.16(3)
X4	4	0.23(4)	→	0.19(3)
X5	4	0.23(4)	→	0.22(3)
X6	4	0.13(4)	→	0.19(3)
Avg.		0.175		0.175
σ_6		0.05		0.03
		Ia3d		
Y	16	0.88	→	0.88
		$I\bar{1}$		
Y1	2	0.04(2)	→	0.12(2)
Y2	2	0.19(2)	→	0.13(2)
Y3	2	0.00(2)	→	0.10(2)
Y4	2	0.15(2)	→	0.09(2)
Y5	2	0.07(2)	→	0.13(2)
Y6	2	0.16(2)	→	0.10(2)
Y7	2	0.15(2)	→	0.11(2)
Y8	2	0.12(2)	→	0.10(2)
Avg.		0.11		0.11
σ_8		0.06		0.03

Note: X sites contain Ca and Fe, and Y sites contain Al and Fe. Standard deviations of last significant figures are given in parentheses.

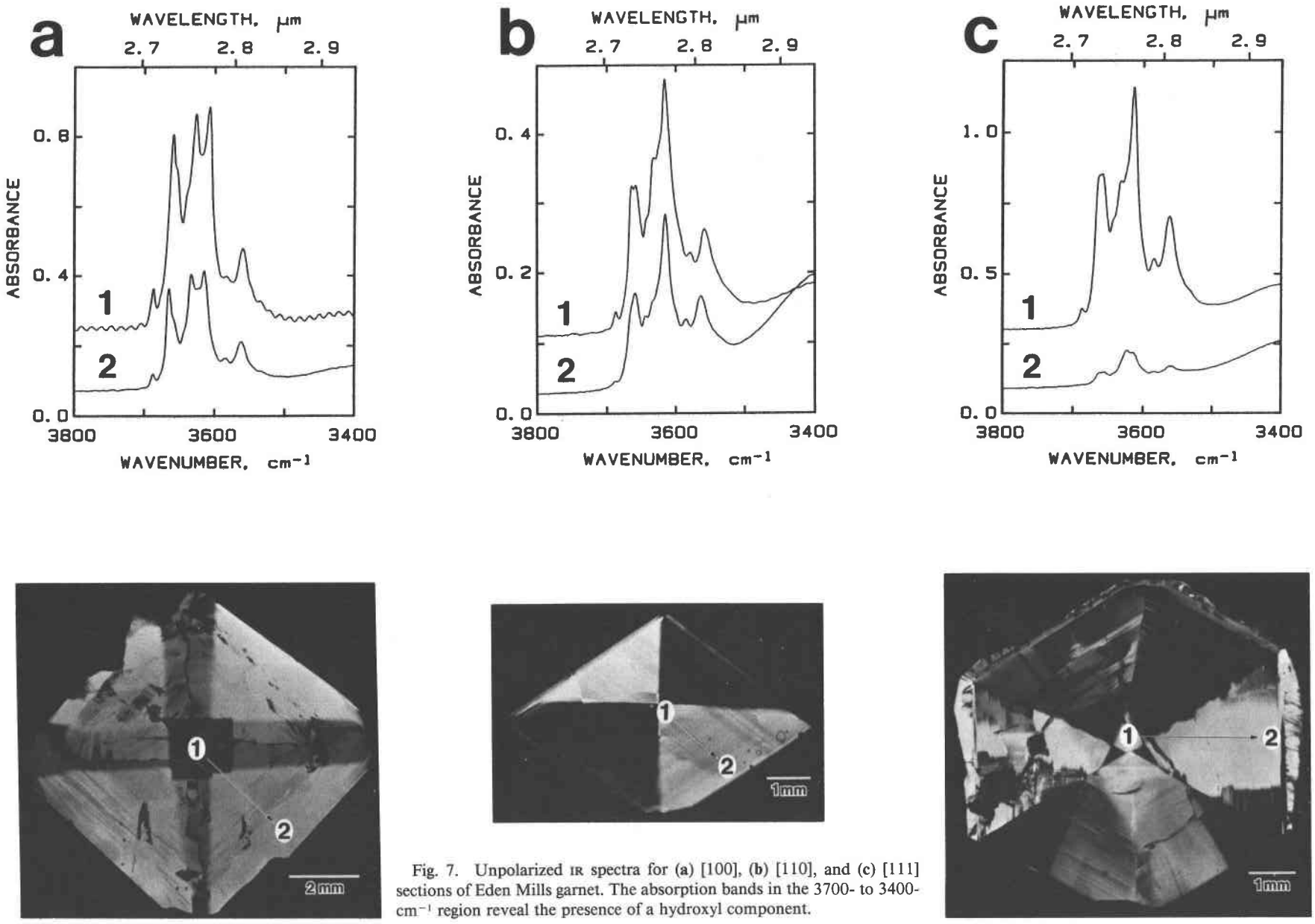

Fig. 7. Unpolarized IR spectra for (a) [100], (b) [110], and (c) [111] sections of Eden Mills garnet. The absorption bands in the 3700- to 3400-cm^{-1} region reveal the presence of a hydroxyl component.

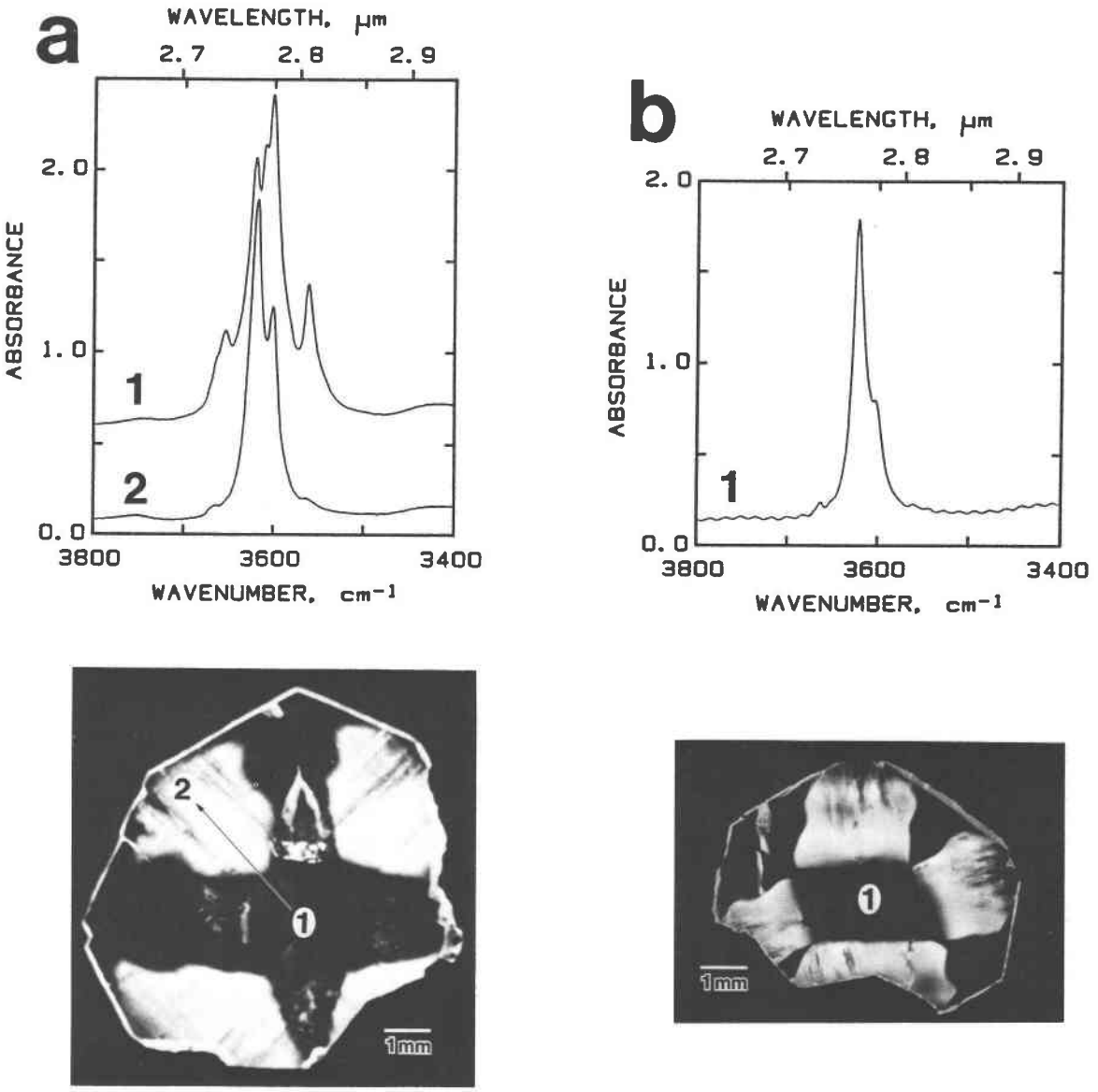

Fig. 8. Unpolarized IR spectra for (**a**) [100] and (**b**) [110] sections of Asbestos garnet. The absorptions are different from those observed in crystals from Eden Mills.

entation dependent, (2) different absorptions are observed for crystals from the two localities, and (3) the intensity of absorption varies from point to point in a sample, but tends to decrease from core to rim. These results show that the distribution of OH groups is variable in garnet and that the Eden Mills and Asbestos samples are noncubic with respect to OH orientation. The OH groups presumably enter the structure via the hydrogarnet substitution: $4(OH^-) = SiO_4^{4-}$ (Aines and Rossman, 1984; Rossman and Aines, 1986). The water content appears to decrease continuously as crystal growth proceeds, but may rise dramatically in the final stages.

Polarized IR spectra (Figs. 9 and 10) indicate anisotropic absorptions at various points in the two samples. Maximum and minimum absorptions are shown in the spectra where appropriate. The anisotropy in the spectra suggests a noncubic distribution of OH groups that presumably contribute to the optical birefringence. The polarized spectra from the two twin sectors in the Eden Mills {110} section are identical. Maximum absorption occurs at 0° in both sectors, not at the optical extinction directions (±16° in this sample). Consequently, a low-symmetry distribution of OH groups may explain the optical anisotropy, but cannot account for the observed sector twinning.

The unheated, anisotropic Eden Mills sample shows a definite hydroxyl component. After annealing at 870 °C, the quenched sample, now isotropic, no longer contained

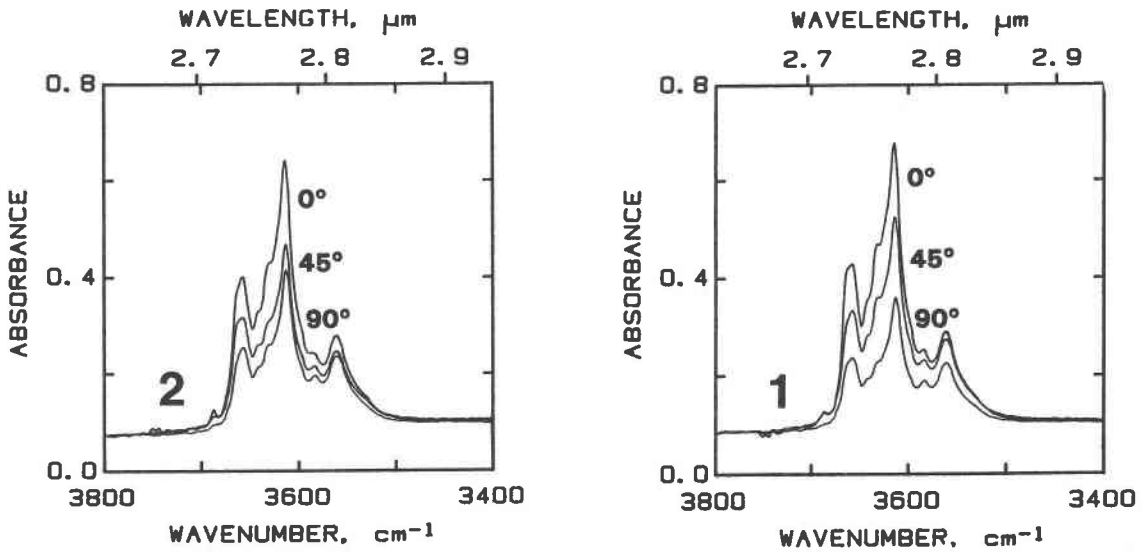

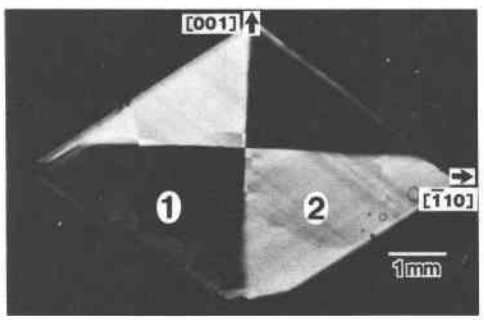

Fig. 9. Polarized IR spectra for the [110] section of Eden Mills garnet shown in Fig. 7b. Anisotropic absorptions are observed at various places in the sample, indicating a noncubic distribution of OH groups. Maximum absorption occurs when the polarizer is vertical (0°), i.e., parallel to [001] of the crystal. Minimum absorption occurs when the polarizer is rotated 90° from vertical, parallel to [$\bar{1}$10].

a hydroxyl component (Fig. 11). In another experiment in which an Eden Mills sample was annealed at 800 °C, the water was also lost, but the sample remained anisotropic indicating that a hydroxyl component cannot be the sole cause for the anisotropy. Factors such as cation ordering must also be important.

Manning and Tricker (1977) proposed a link between the distribution of Fe^{3+} and OH groups. Large half-widths of ferric absorptions in Mössbauer spectra reflect local disorder around octahedral Fe^{3+}. This disorder is attributed to replacement of SiO_4^{4-} by $4(OH^-)$ in next-nearest-neighbor tetrahedral sites.

The substitution of monovalent cations for Ca on the dodecahedral positions may also influence the orientation of OH groups. For example, small amounts of Na occur in most grandite garnets. A coupled replacement of $(Ca^{2+} + O^{2-})$ by $(Na^+ + OH^-)$ may exist to achieve local electrostatic charge balance.

→

Fig. 10. Polarized IR spectra for the [100] section of Asbestos garnet shown in Fig. 8a. Absorptions are shown for polarizer angles of 0° (vertical), 45°, and 90°. Isotropic and anisotropic absorptions are observed, suggesting both cubic and noncubic distributions of OH groups. The absorptions vary throughout the sample, but in an unexpected way. Isotropic absorptions occur in the birefringent sectors (points 1 and 2), whereas anisotropic absorptions occur in the dark cross region (points 3–5). For the latter, maximum absorption occurs when the polarizer is either at 0° (points 3 and 4; parallel to [001] of the crystal) or at 90° (point 5; parallel to [010]).

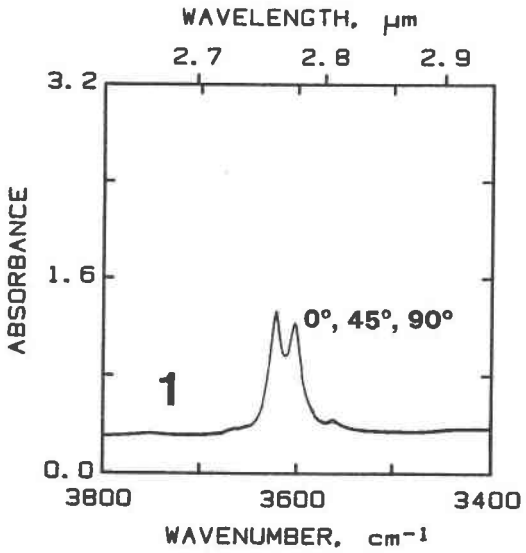
WAVELENGTH, μm
2.7
2.8
2.9
3.2
1.6
0.0
ABSORBANCE
0°, 45°, 90°
1
3800
3600
3400
WAVENUMBER, cm⁻¹

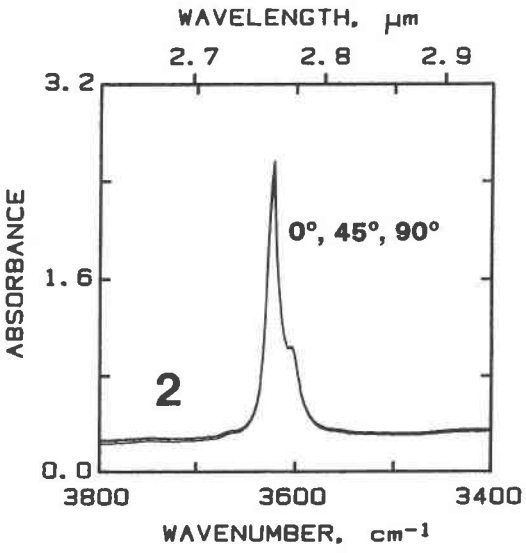
WAVELENGTH, μm
2.7
2.8
2.9
3.2
1.6
0.0
ABSORBANCE
0°, 45°, 90°
2
3800
3600
3400
WAVENUMBER, cm⁻¹

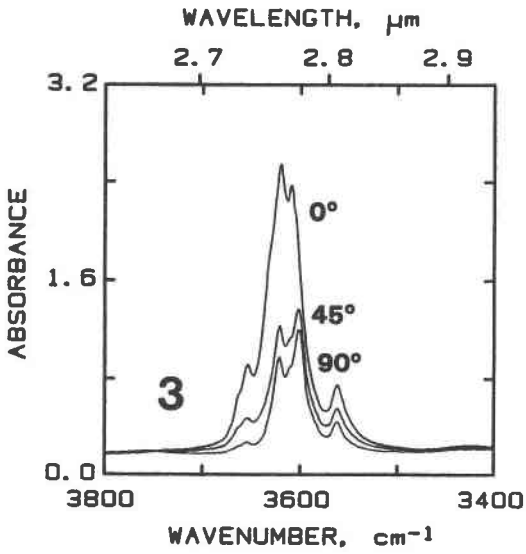
WAVELENGTH, μm
2.7
2.8
2.9
3.2
1.6
0.0
ABSORBANCE
0°
45°
90°
3
3800
3600
3400
WAVENUMBER, cm⁻¹

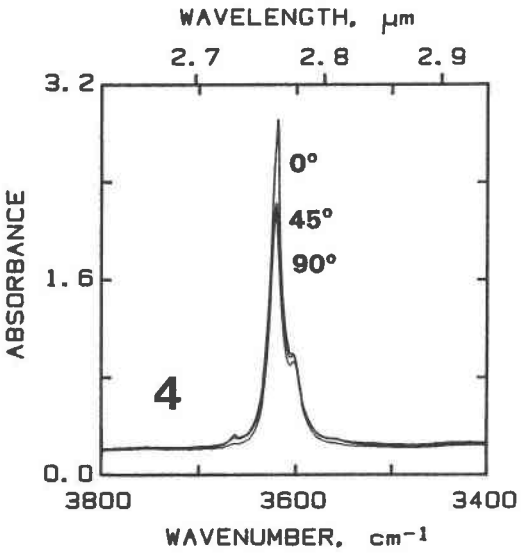
WAVELENGTH, μm
2.7
2.8
2.9
3.2
1.6
0.0
ABSORBANCE
0°
45°
90°
4
3800
3600
3400
WAVENUMBER, cm⁻¹

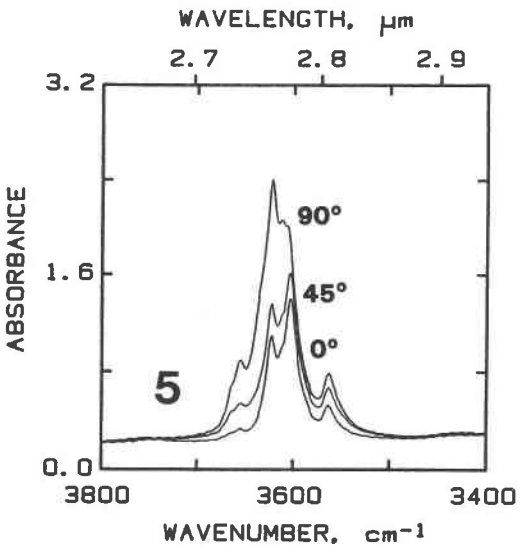
WAVELENGTH, μm
2.7
2.8
2.9
3.2
1.6
0.0
ABSORBANCE
90°
45°
0°
5
3800
3600
3400
WAVENUMBER, cm⁻¹

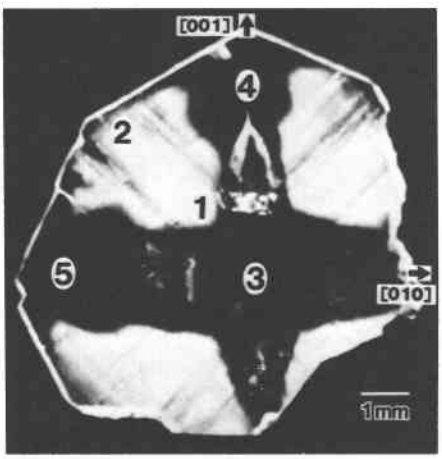
[001]
4
2
1
5
3
[010]
1mm

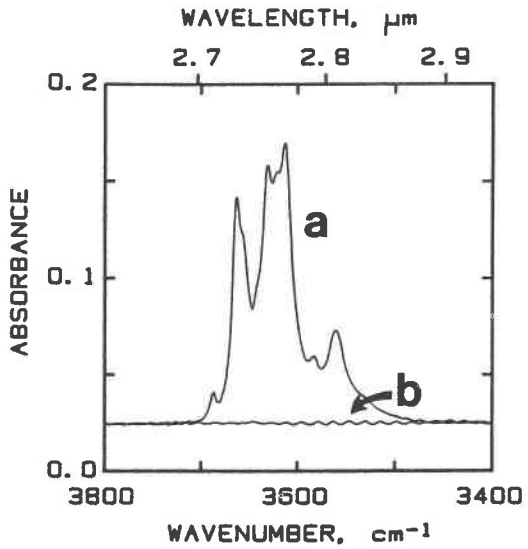

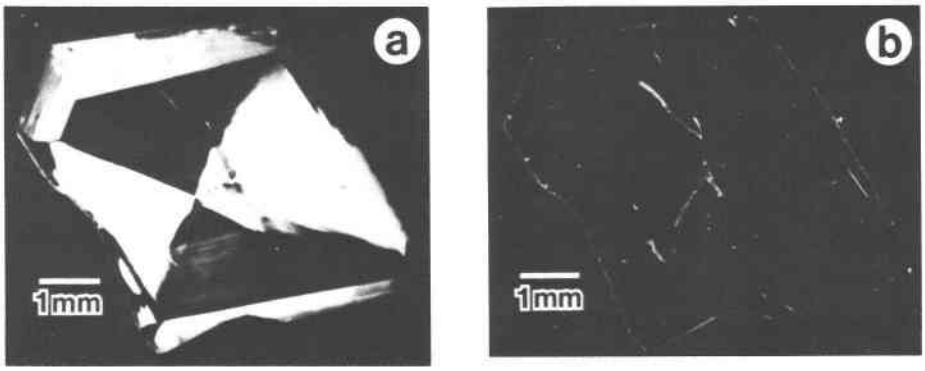

Fig. 11. Unpolarized IR spectra for a [110] section of Eden Mills grossular (**a**) before and (**b**) after annealing. Samples heated to 870 °C lose their water and become isotropic. However, samples heated to 800 °C also lose their water but remain birefringent.

TEM RESULTS

Foils were prepared from thin sections cut parallel (Fig. 12a) and perpendicular (Figs. 12b and 12c) to the {110} surfaces of the Eden Mills grossular. Ar-atom milling was used to perforate the foils. The edges around the holes were too thin to display birefringence. Boundaries between sectors and lamellae had to be visually traced from thick regions to the thin edges.

Extended defects occur in birefringent Eden Mills grossular and are concentrated at the sector boundaries (Figs. 13 and 14; see also Allen et al., 1987). The defects may provide indirect evidence for ordering. Strain presumably results from lattice mismatch across differently ordered layers of atoms, producing defects at the boundaries.

No direct evidence for ordering is revealed in the high-resolution TEM (HRTEM) images of the birefringent garnet (Fig. 15). Images were obtained with a JEOL 4000EX microscope—a 400-keV instrument with a structure resolution of ~1.7 Å. The minor structural variations responsible for the reduction in symmetry are apparently too subtle to be recognized in these high-resolution images. Turner (1978) used HRTEM to study garnets of several compositions, including the triclinic garnet from Munam, Korea, examined by Takéuchi, but no evidence for ordering was detected.

Selected-area electron-diffraction (SAED) experiments were done with a Philips 400T electron microscope operated at 120 kV. The SAED patterns were obtained using a field-limiting aperture 10 μm in diameter. The patterns of Eden Mills garnet also show no evidence of a departure from cubic symmetry. The planar symmetries of the zero-order SAED patterns are $4mm$, $2mm$, and $6mm$. Only a few weak diffractions violating extinction criteria for space group $Ia3d$ were observed, and these can be attributed to multiple diffraction.

Convergent-beam electron diffraction (CBED) was also

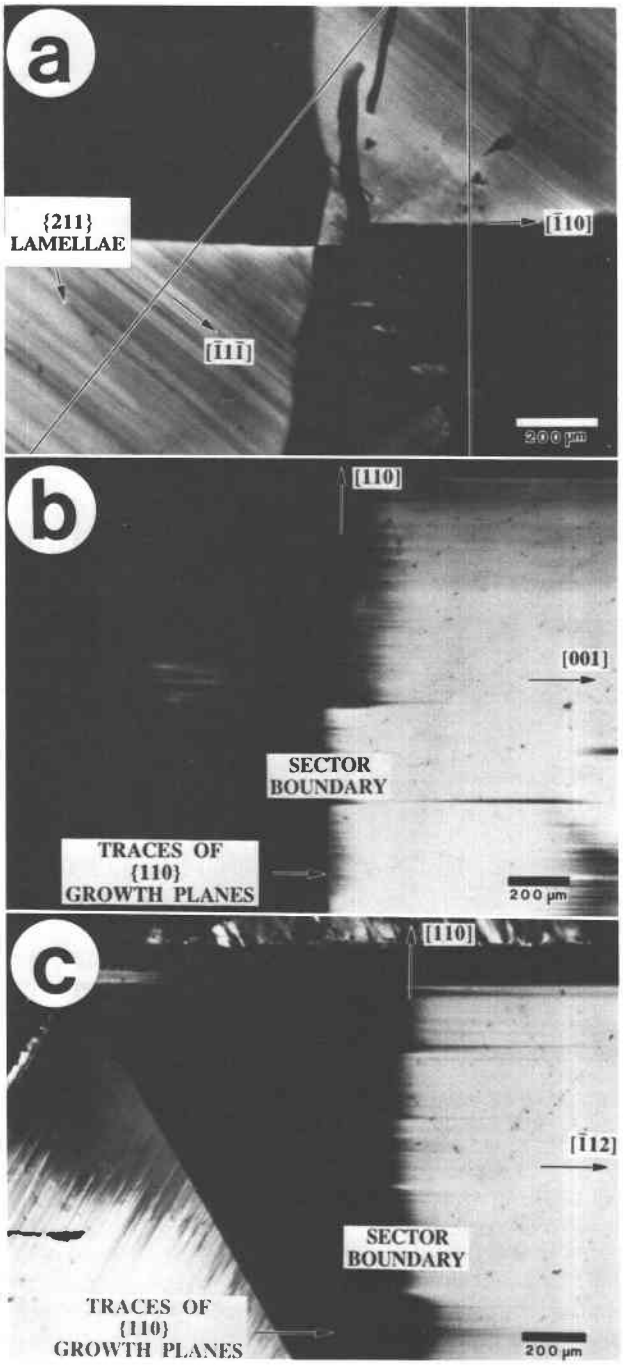

Fig. 12. (**a**) [110] section of Eden Mills grossular showing where perpendicular sections were cut to expose stacks of {110} growth surfaces. {211} lamellae are thought to be traces of former growth steps. (**b**) and (**c**) are [$\bar{1}$10] and [$\bar{1}$1$\bar{1}$] sections, respectively, showing traces of {110} growth surfaces in different sectors. The black and white alternation is presumably caused by changes in optical orientation of differently ordered layers of atoms.

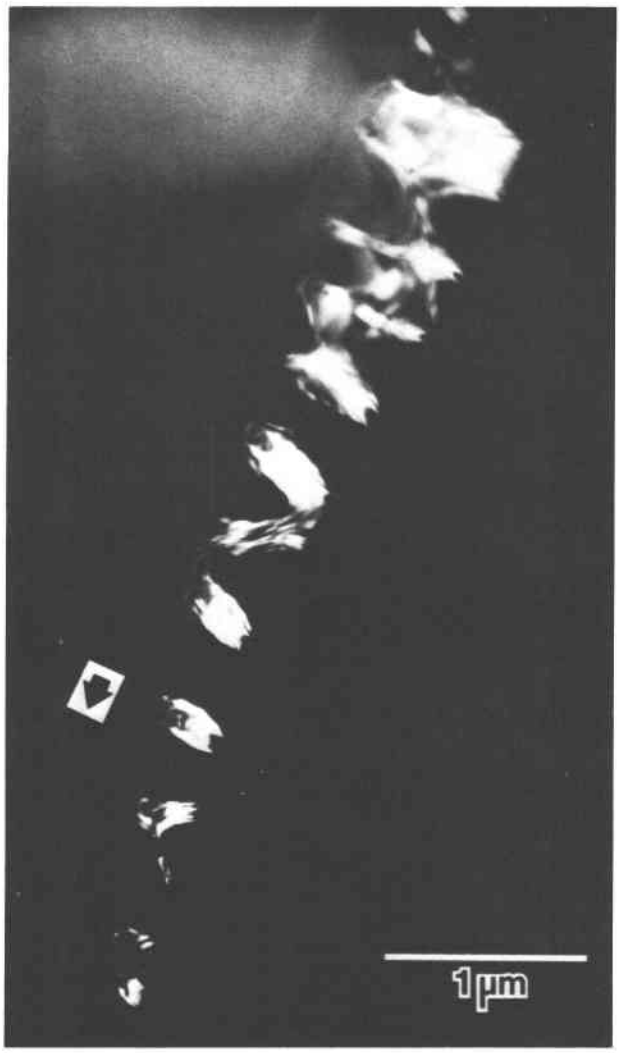

Fig. 13. Helical edge dislocation in anisotropic garnet. The arrow shows the stacking direction of {110} growth layers.

used to determine the symmetry of birefringent sectors in Eden Mills grossular. With CBED, a highly convergent electron beam is focused onto a small area of the sample. Discs of intensity are produced rather than the diffraction spots obtained with parallel illumination in SAED. Sharp lines may occur within the discs as a result of elastic scattering by the planes in higher-order Laue zones (HOLZs). For a amore complete description of the CBED method, see Steeds (1979).

CBED patterns were obtained from several 1000–2000-Å thick regions in the atom-milled foils using a 400-Å probe. Experiments were done both at room temperature (25 °C) and liquid N_2 temperature (−196 °C). Cooling the specimen increases HOLZ line visibility by reducing contamination and beam heating.

Despite the high spatial resolution and great detail in the diffraction discs, CBED failed to provide evidence of a reduction from cubic symmetry in these garnets. The [100]

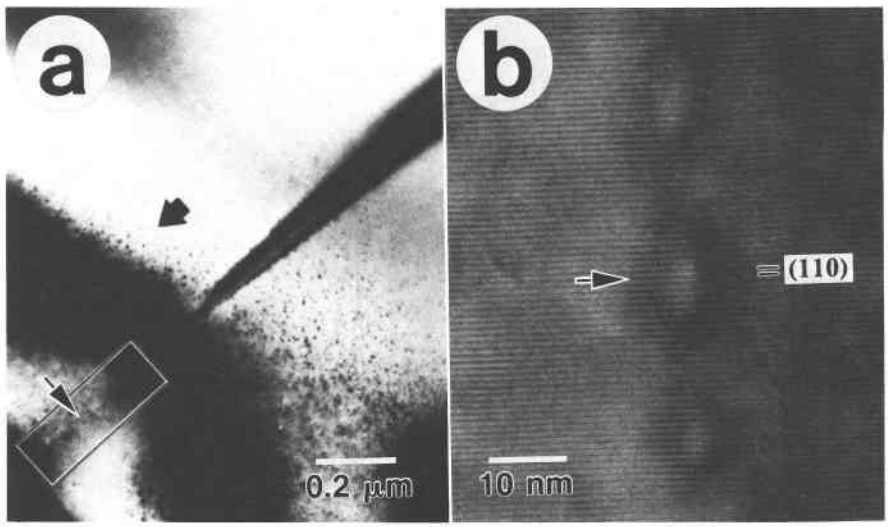

Fig. 14. (**a**) Stacking fault connecting trapped partial dislocations. The arrow indicates the stacking direction of {110} growth layers. A trail of dislocations occurs at the end of the fault. (**b**) HRTEM image of the area enclosed by the box in (**a**). The dislocations are being expelled from the faulted region.

patterns show symmetry $4mm$ for the whole pattern and for the bright-field disc (Fig. 16a), whereas the [110] patterns show symmetry $2mm$ (Fig. 16b) and [111] patterns show symmetry $3m$. These symmetries correspond to diffraction groups that are common only to point group $m3m$. Even at liquid N_2 temperatures, the HOLZ lines indicate cubic symmetry.

CBED falls short in its ability to detect small structural perturbations caused by partial ordering or the presence of trace amounts of impurities. Optical methods seem to be a more sensitive measure of detecting such changes. For example, ordering of OH and F is believed to be responsible for the anomalous optical properties of topaz, but Neder (1985) concluded that CBED was insensitive to the ordering of such light atoms of similar atomic number in the presence of heavier atoms.

CBED also appears to be insensitive to ordering in near–end members when only minor or trace amounts of heavy atoms such as Fe are present among lighter atoms. At least this seems to be true in Ca-Al silicates, many of which exhibit anomalous optical properties related to the presence of impurities. Like grossular, vesuvianite and clinozoisite containing small amounts of Fe and Mn exhibit anomalous optical behavior, but again CBED patterns show no evidence of a symmetry reduction.

Discussion

Optical anisotropy in near-end-member grossular is caused by a variety of mechanisms that occur simultaneously. One mechanism involves partial ordering of Al-Fe^{3+} on the octahedral positions or Ca-Fe^{2+} on the dodecahedral positions. Grossular crystals are composed of triclinic sectors that are twin-related, yielding cubic pseudosymmetry. Ordering presumably takes place during crystal growth and is determined by the two-dimensional atomic arrangement exposed on side faces of growth steps at the surface (Akizuki, 1984). The clear correlation between surface features and internal textures strongly suggests that the internal textures of garnet from Eden Mills formed during growth, not by a phase transition after growth.

A growth model to explain the sector twinning is illustrated in Figure 17. On the {110} growth surfaces, octahedra lie along {211} planes. The {110} surfaces enlarge by filling octahedra in these planes. Twofold rotational symmetry is essentially maintained as growth proceeds in two dimensions. As a growth layer forms, the crystal keeps the same face exposed at the surface at all times, leading to the formation of reflection twins. Lamellar features are thought to be former growth steps that mark small changes in composition, ordering scheme, or degree of ordering. Slight lattice mismatch results, producing strain in the crystal.

The difference in the sizes of the two ions is probably an important factor relating to ordering. Al, being slightly smaller than Fe^{3+} (0.53 and 0.65 Å, respectively), presumably occupies the smallest octahedral void on the surface of the growing crystal. If a preference develops for a particular site, a two-dimensionally ordered structure results. The alignment of magnetic moments of Fe^{3+} sublattices may be an important factor in this regard (Balestrino et al., 1986). Minimizing the structure energy is the ultimate driving force that determines how Al and Fe^{3+} are distributed, which in turn can alter the arrangement of the remaining ions.

There can also be a growth-induced preferential pair (short-range) ordering between cations in the octahedral Y site (Al or Fe^{3+}) and their nearest neighbor in the dodecahedral X site (Ca, Fe^{2+}, Mn, Na, or Mg). The ordering of OH groups can also be involved. Once an ordering

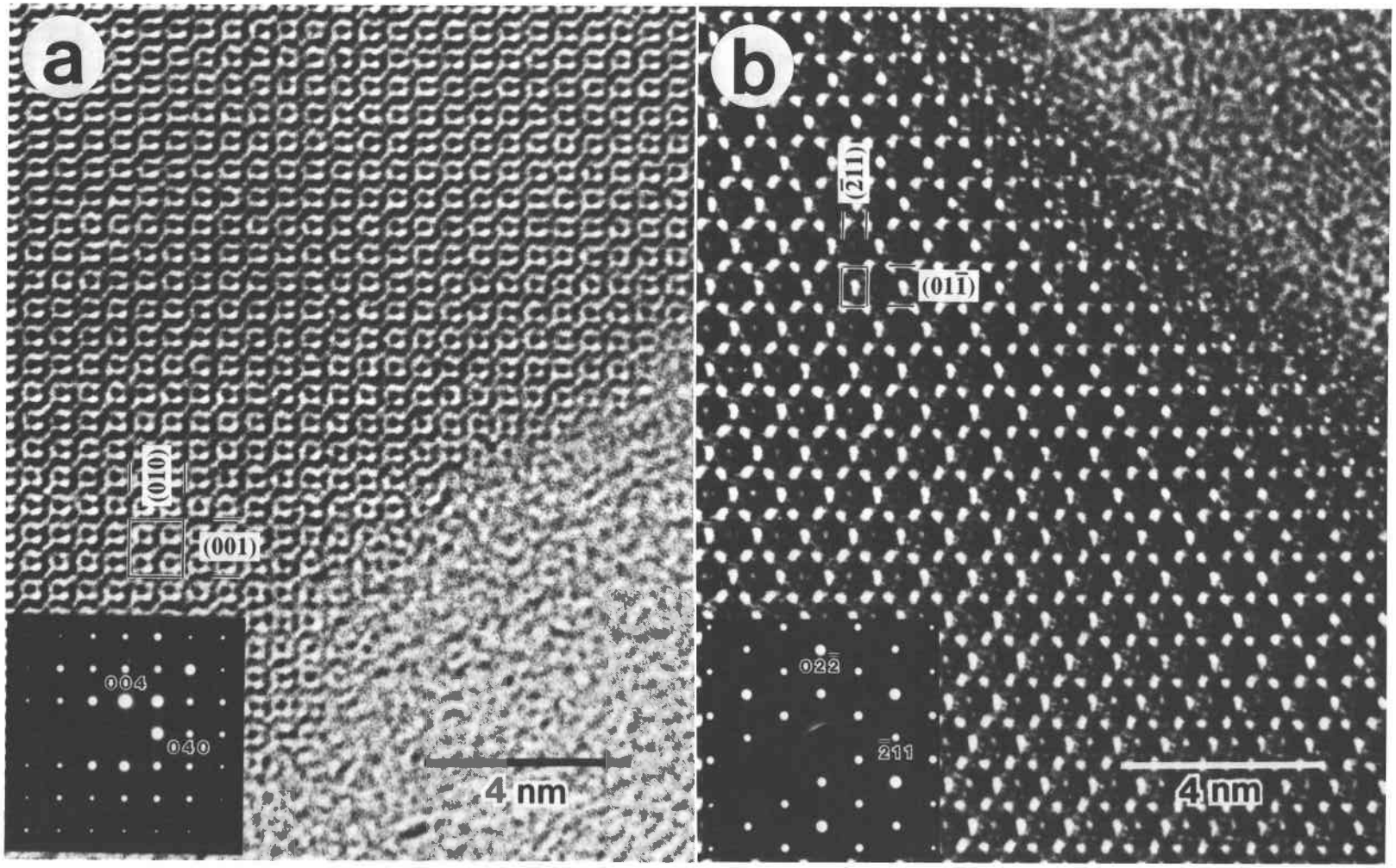

Fig. 15. (**a**) [100] and (**b**) [111] HRTEM structure images of anisotropic Eden Mills garnet. No contrast changes are observed that can be attributed to changes in composition or ordering scheme.

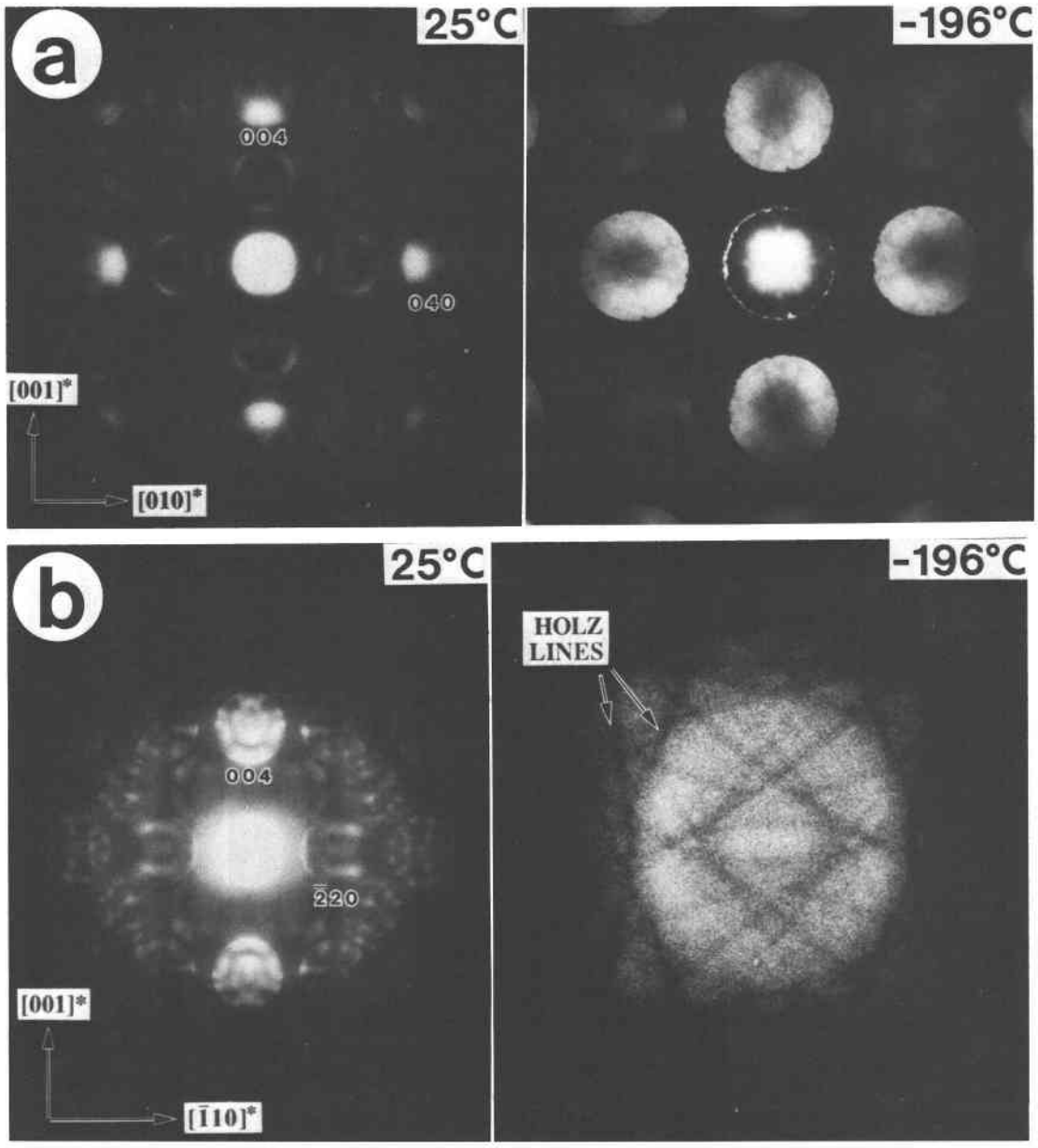

Fig. 16. (a) [100] and (b) [110] CBED patterns from ordered growth sectors in Eden Mills garnet. Cubic symmetry is indicated.

scheme is adopted during growth, it is not likely to change as long as the influx of cations to the surface remains the same, and the temperature and growth rate remain fairly constant. An analogous pair ordering occurs in synthetic rare-earth-element garnets (YAG-YIG) to produce noncubic magnetic anisotropy (Callen, 1971; Rosencwaig et al., 1971).

On heating, an anisotropic garnet becomes increasingly disordered until it loses its birefringence and becomes cubic. The metastable ordered structures produced on surfaces during growth are obliterated on heating. The Al:Fe^{3+} ratio and the degree of ordering are probably important factors in controlling the kinetics of the transition (Takéuchi et al., 1982).

In some garnets, the order-disorder transformation is reversible. Hariya and Kimura (1978) reported that inverted cubic garnets regained their birefringence after annealing at lower temperatures. In the present study, the heated Eden Mills garnets remained isotropic when cooled rapidly by quenching and when cooled slowly (−20 °C/h) to room temperature.

OH groups are distributed in a noncubic manner explaining, in part, the optical anisotropy in Eden Mills and Asbestos garnets. No obvious relationships exists, how-

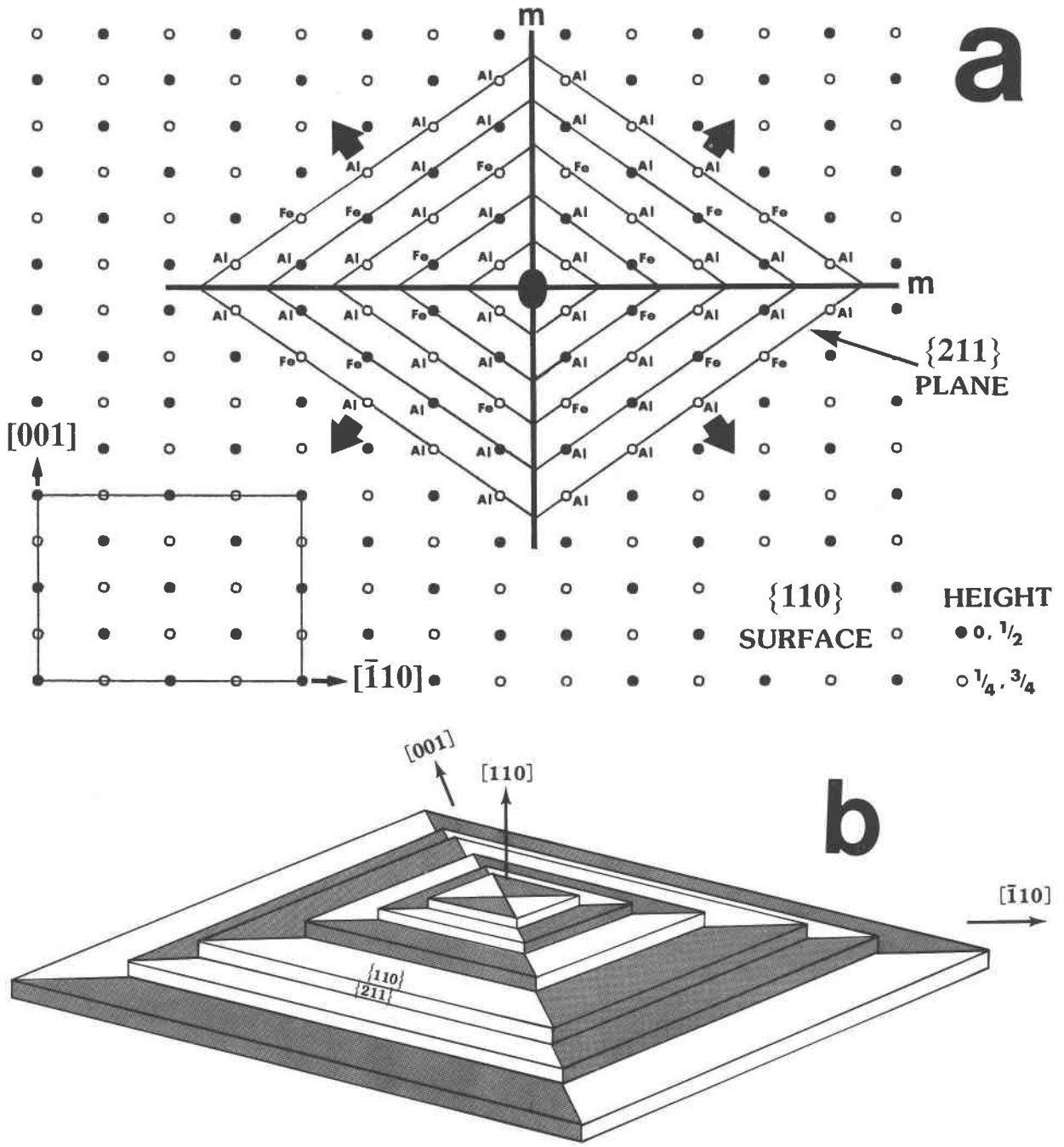

Fig. 17. A model explaining the origin of sector twinning in garnet. (**a**) [110] projection showing only the atoms in octahedral positions; a unit cell is outlined. The octahedral positions lie on {211} planes. {110} surfaces grow in two dimensions as octahedra are filled (arrows). Twofold rotational symmetry is maintained in this process, and twinning keeps the same face exposed on the surface as the crystal grows. (Twin planes are labeled *m*). The ordering scheme may change on the surface during growth, resulting in the development of steps. (**b**) A stack of {110} surfaces with differently ordered sectors. The heights of the steps are exaggerated.

ever, between the polarization direction corresponding to maximum IR absorption and the optical extinction directions of sector twins. Further work is necessary to determine whether a low-symmetry OH orientation is a primary feature or if the OH groups respond to another component that is subject to preferential ordering during growth.

Defect structures have been observed in near-end-member grossular samples cut normal to {110} growth surfaces. Lattice strain results from mismatch arising from

compositional changes (probably involving Fe or trace amounts of OH, Na, Mg, Ti, or Mn) or changes in the ordering scheme or degree of ordering.

As a garnet crystal grows in a hydrothermal environment, changes in temperature or fluid composition are likely to have an effect on its surface structure. One way is by varying the ordering scheme, and another is by altering the chemical composition. Even slight changes can cause lattice mismatch, producing strain in a crystal that is otherwise cubic and thereby reducing the symmetry.

Conclusions

By combining crystallographic techniques, we have explained in part the complex origin of anisotropy in garnet. Optics are more sensitive than X-ray and electron-diffraction methods for detecting slight departures from cubic symmetry. However, optical measurements alone do not provide enough information to determine the cause of the anisotropy. XRD shows subtle cation ordering, and FTIR shows a noncubic distribution of OH groups. HRTEM images show no effects of ordering, but do show sector-boundary defects arising from strain.

Acknowledgments

We thank Victor Young for help with the single-crystal X-ray diffraction experiments, George Rossman for help with the FTIR spectroscopy at Caltech, and John Barry for getting us started on the JEOL 4000EX electron microscope. Rich Reeder provided a highly helpful review. Our appreciation is also extended to John Wheatley and the rest of the staff at the Facility for High Resolution Electron Microscopy in the Center for Solid State Science at A.S.U. This study was supported by NSF grant EAR-8408168.

References cited

Aines, R.D., and Rossman, G.R. (1984) The hydrous component in garnets: Pyralspites. American Mineralogist, 69, 1116–1126.

Akizuki, M. (1984) Origin of optical variations in grossular-andradite garnet. American Mineralogist, 66, 403–409.

Allen, F.M., Smith, B.K., and Buseck, P.R. (1987) Direct observation of dissociated dislocations in garnet. Science, 238, 1695–1696.

Balestrino, G., Paroli, P., and Geller, S. (1986) Growth anisotropy in the Nd-Y and Pr-Y iron garnets. Physical Review B. Condensed Matter, 34, 8104–8106.

Blanc, Y., and Maisonneuve, J. (1973) Sur la biréfringence des grenats calciques. Bulletin de la Société française de Minéralologie et de Cristallographie, 96, 320–321.

Callen, H. (1971) Growth-induced anisotropy by preferential site ordering in garnet crystals. Applied Physics Letters, 18, 311–313.

Chase, A.B., and Lefever, R.A. (1960) Birefringence of synthetic garnets. American Mineralogist, 45, 1126–1129.

Evans, B.W., Johannes, J., Oterdoom, H., and Trommsdorff, V. (1976) Stability of chrysotile and antigorite in the serpentine multisystem. Schweizerische Mineralogische und Petrographische Mitteilungen, 56, 79–93.

Hariya, Y., and Kimura, M. (1978) Optical anomaly garnet and its stability field at high pressures and temperatures. Journal of Faculty of Science, Hokkaido University, Series IV, 18, 611–624.

Hirai, H., and Nakazawa, H. (1986) Visualizing low symmetry of a grandite garnet on precession photographs. American Mineralogist, 71, 1210–1213.

International tables for X-ray crystallography (1974) Vol. IV. Kynoch Press, Birmingham, England.

Kitamura, K., and Komatsu, H. (1978) Optical anisotropy associated with growth striation of yttrium garnet, $Y_3(Al,Fe)_5O_{12}$. Kristallographie und Technik, 13, 811–816.

Lessing, P., and Standish, R.P. (1973) Zoned garnet from Crested Butte, Colorado. American Mineralogist, 58, 840–842.

Manning, P.G., and Tricker, M.J. (1977) A Mössbauer spectral study of ferrous and ferric ion distributions in grossular crystals: Evidence for local crystal disorder. Canadian Mineralogist, 15, 81–86.

Neder, R.B.W. (1985) Sensitivity of convergent-beam electron diffraction to F-OH order-disorder in topaz. M.S. thesis, Arizona State University, Tempe, Arizona.

Rosencwaig, A., Tabor, W.J., and Pierce, R.D. (1971) Pair-preference and site-preference models for rare-earth iron garnets exhibiting noncubic magnetic anisotropies. Physical Review Letters, 26, 779–783.

Rossman, G.R., and Aines, R.D. (1986) Spectroscopy of a birefringent grossular from Asbestos, Quebec, Canada. American Mineralogist, 71, 779–780.

Steeds, J.W. (1979) Convergent beam electron diffraction. In J.J. Hren, J.I. Goldstein, and D.C. Joy, Eds., Introduction to analytical electron microscopy, p. 387–422. Plenum Press, New York.

Takéuchi, Y., and Haga, N. (1976) Optical anomaly and structure of silicate garnets. Proceedings of the Japanese Academy, 52, 228–231.

Takéuchi, Y., Haga, N., Umizu, S., and Sato, G. (1982) The derivative structure of silicate garnets in grandite, Zeitschrift für Kristallographie, 158, 53–99.

Turner, S. (1978) High-resolution transmission electron microscopy of some manganese oxides and silicate minerals. M.S. thesis, Arizona State University, Tempe, Arizona.

Manuscript received July 24, 1987
Manuscript accepted January 20, 1988